

Thermoelectric figure of merit of AlPdRe icosahedral quasicrystals: Composition-dependent effects

Enrique Macia*

Departamento de Física de Materiales, Facultad de Físicas, Universidad Complutense de Madrid, E-28040 Madrid, Spain

(Received 14 January 2004; revised manuscript received 4 March 2004; published 26 May 2004)

In this work we present a theoretical study on the composition dependence of the thermoelectric figure of merit (ZT) of icosahedral AlPdRe quasicrystals. From our study we conclude that band-structure effects play a significant role in determining the thermoelectric performance of these alloys. By comparing our analytical results with available experimental data of transport coefficients we discuss the most appropriate stoichiometries for thermoelectric applications, concluding that (i) those samples whose Fermi level is located at the pseudogap's minimum exhibit very small ZT values, and (ii) relatively large ZT values are expected for those samples exhibiting narrow features in the density of states close to the Fermi level.

DOI: 10.1103/PhysRevB.69.184202

PACS number(s): 61.44.Br, 71.20.-b, 72.10.-d

I. INTRODUCTION

During the last few years we have witnessed an increasing interest in searching for novel thermoelectric materials (TEM's).¹ Among the proposed candidates quasicrystals (QC's) occupy a singular position, since these alloys may naturally fit the Slack's requirements for a material belonging to the "electronic crystal/phonon glass" class.^{2,3} In fact, the *electronic transport properties* of quasicrystalline alloys exhibit unusual composition and temperature dependences, exhibiting more semiconductorlike than metallic character.⁴ Thus, their electrical conductivity steadily increases as the temperature increases up to the highest temperatures of measurement, and it is extremely sensitive to minor variations in the sample composition.^{5,6} This sensitivity to the sample stoichiometry is also observed in the Seebeck coefficient, and resembles doping effects in semiconductors. In addition, thermopower has large values when compared to those of usual metallic systems and its temperature dependence exhibits well-defined extrema and sign reversals in some instances.⁷⁻¹⁰ On the other hand, the *thermal conductivity* of QC's is unusually low for a metallic alloy and it is mainly determined by the lattice phonons, rather than by the charge carriers, over a wide temperature range.¹¹⁻¹³

Consequently, according to their transport properties, quasicrystalline alloys are marginally metallic and should be properly located at the *border line* between metals and semiconductors.⁴ In fact, it has been recently pointed out that the electrical conductivity of *i*-AlPd(Mn,Re) QC's may be strongly dependent on the bonding nature of their constitutive icosahedral clusters, so that small changes in the cluster structure may induce a metallic-covalent bonding conversion.¹⁴ Thus, QC's bridge the gap between metallic materials and semiconducting ones, occupying a very promising position in the quest for novel TEM's.

The efficiency of thermoelectric devices depends on the transport coefficients of the constituent materials and it can be expressed in terms of the figure of merit (FOM) given by the dimensionless expression

$$ZT \equiv \frac{\sigma S^2 T}{\kappa_e + \kappa_{ph}}, \quad (1)$$

where T is the temperature, $\sigma(T)$ is the electrical conductivity, $S(T)$ is the Seebeck coefficient, $\kappa_e(T)$ is the charge carrier contribution to the thermal conductivity, and $\kappa_{ph}(T)$ is the lattice contribution to the thermal conductivity.

According to their chemical composition QC's can be grouped into several families. In Table I we list the transport coefficient values for those representatives yielding the best FOM values at room temperature. From the listed data we appreciate a progressive trend towards larger values of ZT , resulting from the synthesis of suitable QC's. Furthermore, significantly enhanced FOM values are obtained at higher temperatures. Thus we have $ZT=0.25$ for *i*-AlPdMn samples¹⁵ at $T=550$ K, $ZT=0.11$ for *i*-Al₇₁Pd₂₀Re₉ samples¹⁶ at $T=660$ K, and $ZT=0.15$ for *i*-Al₇₁Pd₂₀(Re_{0.45}Ru_{0.55})₉ samples¹⁷ at $T=700$ K.

Along with these experimental results, additional evidence on the potential of QC's as TEM's comes from theoretical considerations as well. On the one hand, the electronic structure of QC's properly satisfies the optimal electronic structure requirements proposed by Mahan and Sofo.^{20,21} In fact, the presence of a pronounced pseudogap at the Fermi level²²⁻²⁵ minimizes the density of states (DOS) background contribution, while the existence of narrow features in the DOS^{26,27} increases the probability of finding a sharp feature located at the proper place. On the other hand, the character-

TABLE I. Room temperature transport coefficient values for different quasicrystalline families.

Sample	σ ($\Omega^{-1} \text{ cm}^{-1}$)	S ($\mu\text{V K}^{-1}$)	κ ($\text{W m}^{-1} \text{ K}^{-1}$)	ZT
AlCuRu	250 ^a	27 ^a	1.8 ^b	0.003
AlCuFe	310 ^a	44 ^a	1.8 ^c	0.01
CdYb	7000 ^d	16 ^d	4.7 ^d	0.01
AlCuRuSi	390 ^a	50 ^a	1.8 ^b	0.02
AlPdRe	175 ^e	95 ^e	0.7 ^e	0.07
AlPdMn	640 ^f	85 ^f	1.6 ^f	0.08

^aRef. 7.^bEstimated.^cRef. 13.^dRef. 19.^eRef. 18.^fRef. 10.

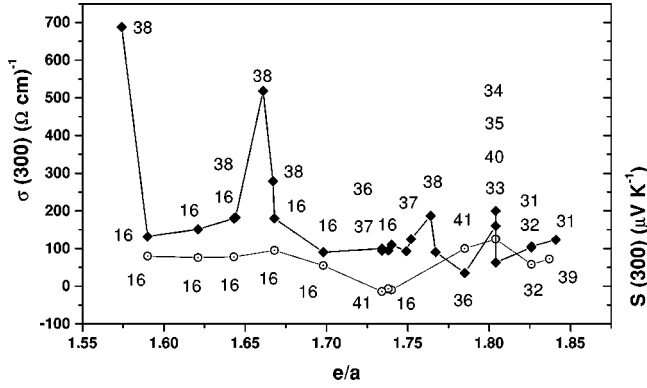


FIG. 1. Room-temperature electrical conductivity (diamonds) and Seebeck coefficient (dotted circles) as a function of the e/a ratio for several i -AIPdRe samples as reported in the literature. The labels indicate the reference number.

istic quasiperiodic order present in QC's may significantly enhance the role of the phonon drag contribution through quasi-Umklapp processes.²⁸

Motivated by these results, we have recently presented a theoretical analysis on the possible use of QC's as potential TEM's.^{21,29} In our previous works we considered a simple electronic model, based on correlated δ -Dirac functions, and we focused on the temperature dependence of the transport coefficients. The aim of this work is to further elaborate these earlier results in order to gain an additional insight into the composition dependence of transport properties and their influence in the resulting FOM. To this end, we shall consider a *realistic model* for the spectral conductivity of QC's, originally proposed by Landau and Solbrig.^{30,31}

The paper is organized as follows. In Sec. II we consider relevant experimental data concerning the composition dependence of different transport coefficients of i -AIPdRe QC's and report on an empirical correlation between the FOM value and the electronic structure of the sample. In Sec. III, discuss this empirical trend in terms of a closed analytical expression for the FOM as a function of a set of phenomenological coefficients. Finally, in Sec. IV we summarize the main conclusions of this work.

II. TRANSPORT PROPERTIES OF AIPdRe ICOSAHEDRAL QUASICRYSTALS: COMPOSITION DEPENDENCE CORRELATIONS

By inspecting Table I we realize that the most promising QC's for thermoelectric applications belong to the AIPd(Mn,Re) family. In this work we will focus on the AIPdRe system. Systematic investigations indicate that their electrical transport properties exhibit a remarkable composition dependence, while thermal conductivity is less sensitive to the sample's composition.^{32–39} In Fig. 1 and Table II we summarize room-temperature electrical conductivity, thermoelectric power, and thermal conductivity data reported for several i -AIPdRe samples. The alloys are arranged according to their average valence electron per atom ratio, e/a . This value is calculated from the alloy's nominal composition⁴³ by assuming the valence values Al = +3.00, Pd=0.00, and

TABLE II. Room-temperature thermal conductivity of several i -AIPdRe samples as a function of their e/a ratio and rhenium content.

Sample	e/a	Re (%)	κ ($\text{W m}^{-1} \text{K}^{-1}$)
Al ₇₀ Pd _{22.5} Re _{7.5}	1.826	7.5	1.56 ^a
Al _{68.5} Pd _{22.9} Re _{8.6}	1.740	8.6	1.16 ^b
Al _{67.7} Pd _{23.2} Re _{9.1}	1.698	9.1	0.86 ^b
Al _{67.8} Pd _{22.2} Re _{10.0}	1.668	10.0	0.76 ^b

^aRef. 33.

^bRef. 16.

Re = -3.66. The apparent negative valence of transition-metal atoms can be understood in terms of $sp-d$ hybridization effects,⁴⁴ within the Hume-Rothery alloy picture proposed by Raynor.⁴⁵

Making use of the data plotted in Fig. 1, we obtain the room-temperature power factor (σS^2) curve shown in Fig. 2 (main frame). In the inset we plot the linear fitting corresponding to the thermal conductivity data listed in Table II. We see that $\kappa = \kappa_e + \kappa_{ph}$ linearly increases (decreases) as the e/a ratio (Re content) is progressively increased. Both trends, respectively, correlate with (i) a progressive increase of the charge carrier contribution to the thermal conductivity by increasing e/a and, (ii) a progressive degradation of the phonon thermal modes due to an increasing concentration of heavier Re atoms in the quasilattice.

In the inset of Fig. 3 we compare the room-temperature ZT values listed in Table III with the power factor curve shown in Fig. 2 (main frame). As expected from the linear κ dependence on e/a , the ZT curve closely resembles the power factor curve. Both curves exhibit a well-defined minimum located at about $e/a \approx 1.74$, hence confirming the expectations raised by Kirihaara and Kimura (cf. Fig. 7 in Ref. 16). The empirical trends illustrated in Figs. 2 and 3 suggest that band-structure effects might play an important role in determining the thermoelectric efficiency of AIPdRe QC's.

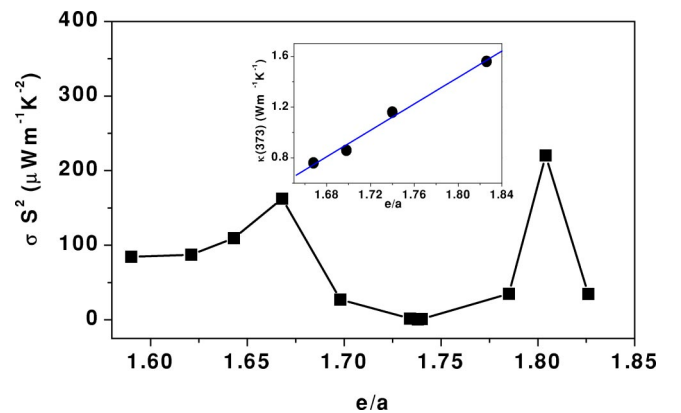


FIG. 2. Composition dependence of the room-temperature thermopower factor of several i -AIPdRe samples shown in Fig. 1 (main frame). Composition dependence of the room-temperature thermal conductivity of the i -AIPdRe samples listed in Table II (inset). The linear regression fit reads $\kappa = (5.2 \pm 0.4)[e/a] - (7.9 \pm 0.6)$, with $r = 0.9908$.

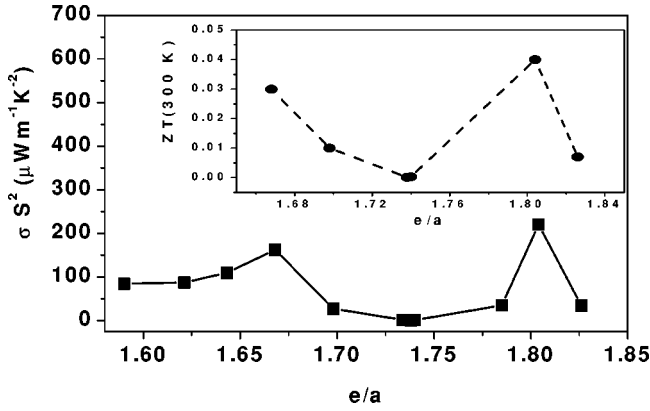


FIG. 3. Comparison between the room-temperature thermopower factor (main frame) and the thermoelectric figure of merit (inset) as a function of the e/a ratio for several i -AlPdRe samples.

In fact, according to electronic stability considerations, based on the Hume-Rothery mechanism,⁴⁶ the ratio $e/a=1.74$ is close to that expected for most stable samples in the AlPdRe system. On the other hand, the peaks appearing at both sides of the minimum are probably related to hybridization effects involving d -Re states. Then, the shape of the ZT curve indicates that those samples whose Fermi level is located at the minimum of the pseudogap, do not exhibit the best thermoelectric properties. Instead, we should consider samples which are near neighbors in the ternary phase diagram, but with a slightly different stoichiometric composition, able to shift the Fermi level from this minimum towards one of the peaks which flank it.

To further substantiate this physical scenario we consider the phenomenological coefficient^{47,48}

$$\xi_1 = \frac{1}{2} \left(\frac{d \ln \sigma(E)}{dE} \right)_{E=\mu}, \quad (2)$$

which is related to the electronic structure of the sample close to the Fermi level, μ , by means of the spectral conductivity function $\sigma(E) = e^2 N(E) D(E)$, where $N(E)$ is the DOS and $D(E)$ is the diffusivity of the charge carriers. Hence, we have two different contributions determining the final value of ξ_1 . In our treatment we will assume that the energy dependence of the diffusivity factor is quite smooth as compared with the energy dependence of the DOS, so that, in a first approximation we can confidently skip the

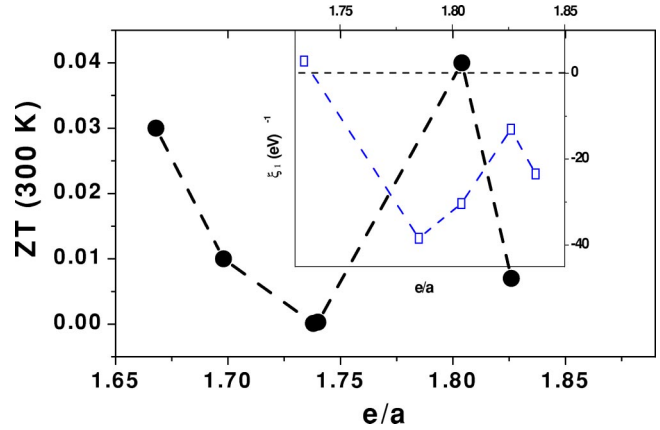


FIG. 4. Comparison between the phenomenological coefficient ξ_1 (inset) and the room-temperature thermoelectric figure of merit (main frame) as a function of the e/a ratio for the i -AlPdRe samples listed in Tables IV and III, respectively.

contribution of the term $N(\mu)(dD/dE)_\mu$ as compared to $D(\mu)(dN/dE)_\mu$ in Eq. (2). This assumption is experimentally supported by (i) low diffusivity estimations (in the range $10^{-6} - 10^{-5} \text{ m}^2 \text{ s}^{-1}$) derived from specific-heat data, using the Einstein relation $\sigma(\mu) = e^2 N(\mu) D_0$,⁹ and (ii) by angle-resolved photoelectron spectra showing flat narrow-band features indicating quite small group velocities for the charge carriers.⁴⁹ In addition, low values for the electronic diffusivity have been obtained in a number of numerical simulations dealing with realistic quasiperiodic systems.⁵⁰

On the other hand, the coefficient ξ_1 can be experimentally determined from the low-temperature slope of the thermoelectric power curve by means of the expression⁴⁸

$$S(T \rightarrow 0) = -2|e| \mathcal{L}_0 \xi_1 T,$$

where $\mathcal{L}_0 = \pi^2 k_B^2 / 3e^2 = 2.44 \times 10^{-8} \text{ V}^2 \text{ K}^{-2}$ is the Lorenz number. In the inset of Fig. 4 we plot the ξ_1 values given in Table IV as a function of the e/a ratio for several samples, and compare them with the ZT values reported in Fig. 3 (main frame). From this figure we conclude that $|\xi_1|$ and ZT values are *directly correlated*. In fact, both ξ_1 and ZT almost vanish at $e/a \approx 1.74$, meanwhile they attain extreme values close to $e/a = 1.79 - 1.80$. Then, the ZT overall behavior can be traced back to the *topology* of the spectral conductivity function close to the Fermi level by means of Eq. (2). In order to gain additional understanding on the nature of such

TABLE III. Room temperature thermoelectric figure of merit of several i -AlPdRe samples.

Sample	Ref.	e/a	σ ($\Omega^{-1} \text{ cm}^{-1}$)	S ($\mu\text{V K}^{-1}$)	κ ($\text{W m}^{-1} \text{ K}^{-1}$)	ZT
Al ₇₀ Pd _{22.5} Re _{7.5}	33	1.826	103	58	1.56	0.007
Al _{70.5} Pd ₂₁ Re _{8.5}	41	1.804	141 ^a	125	1.6 ^b	0.04
Al _{68.5} Pd _{22.9} Re _{8.6}	16	1.740	110	-10	1.16	0.0003
Al _{69.4} Pd _{21.2} Re _{9.4}	16	1.738	95	-7	1.2 ^b	0.0001
Al _{67.7} Pd _{23.2} Re _{9.1}	16	1.698	90	55	0.86	0.01
Al _{67.8} Pd _{22.2} Re _{10.0}	16	1.668	180	95	0.76	0.06

^aMean value from data shown in Fig. 1.

^bEstimated.

TABLE IV. Phenomenological coefficient ξ_1 values for several *i*-AlPdRe samples derived from thermopower curves reported in the literature. The low-temperature slope, a , is related to ξ_1 through the expression $\xi_1 \approx -20.5a[\mu\text{V K}^{-2}]$ (eV) $^{-1}$ (cf. Ref. 48 for more details).

Sample	Ref.	e/a	$a(\mu\text{V K}^{-2})$	ξ_1 (eV) $^{-1}$
Al ₇₁ Pd ₂₁ Re ₈	40	1.837	1.14	-23.43
Al ₇₀ Pd _{22.5} Re _{7.5}	33	1.826	0.64	-13.05
Al _{70.5} Pd ₂₁ Re _{8.5}	41	1.804	1.48	-30.34
Al ₇₀ Pd _{21.4} Re _{8.6}	42	1.785	1.87	-38.37
Al ₇₀ Pd ₂₀ Re ₁₀	42	1.734	-0.14	+2.79

a relationship, in the following section we will obtain an analytical expression for the FOM within the framework of our phenomenological approach.

III. ANALYTICAL TREATMENT

The temperature-dependent transport coefficients can be obtained by means of the Chester-Thellung-Kubo-Greenwood version of the linear response theory.⁵¹⁻⁵³ The central information quantities are the kinetic coefficients

$$\mathcal{L}_{ij}(T) = (-1)^{i+j} \int \sigma(E)(E-\mu)^{i+j-2} \left(-\frac{\partial f}{\partial E} \right) dE, \quad (3)$$

where $f(E, \mu, T)$ is the Fermi-Dirac distribution function. In this formulation all the microscopic details of the system are included in the $\sigma(E)$ function. From the knowledge of the kinetic coefficients one obtains the electrical conductivity

$$\sigma(T) = \mathcal{L}_{11}(T), \quad (4)$$

the thermoelectric power

$$S(T) = \frac{1}{|e|T} \frac{\mathcal{L}_{12}(T)}{\sigma(T)}, \quad (5)$$

and the electronic thermal conductivity

$$\kappa_e(T) = \frac{1}{e^2 T} \mathcal{L}_{22}(T) - T \sigma(T) S(T)^2, \quad (6)$$

in a unified way. As a first approximation we will assume $\mu(T) \approx E_F$. Then, by expressing Eqs. (4)–(6) in terms of the scaled variable $x \equiv (E-\mu)/k_B T$, the transport coefficients can be rewritten as^{21,54,55}

$$\sigma(T) = \frac{J_0}{4}, \quad (7)$$

$$S(T) = -\frac{k_B}{|e|} \frac{J_1}{J_0}, \quad (8)$$

$$\kappa_e(T) = \frac{k_B^2 T}{4e^2} \left(J_2 - \frac{J_1^2}{J_0} \right), \quad (9)$$

where we have introduced the reduced kinetic coefficients

$$J_n(T) = \int x^n \sigma(x) \text{sech}^2(x/2) dx. \quad (10)$$

Plugging Eqs. (7)–(9) into Eq. (1), we get

$$ZT = \frac{J_1^2}{J_0 J_2 - J_1^2 + c^2 J_0 \varphi}, \quad (11)$$

where $c \equiv 2e/k_B$ and $\varphi(T) \equiv \kappa_{ph}(T)/T$. Mahan and Sofo suggested that the best thermoelectric material is likely to be found among materials exhibiting a sharp singularity (Dirac δ function) in the DOS close to the Fermi level.²⁰ Making use of Eq. (10), in that case we get $J_0 J_2 = J_1^2$. According to Eq. (9) this implies that the electronic contribution to the thermal conductivity vanishes identically for all temperatures. This unphysical behavior can be avoided by considering two spectral features in the electronic structure instead of a single one.⁵⁴ Thus, in previous works^{47,48,54,55} we have shown that the $\sigma(T)$, $S(T)$, and $\kappa_e(T)$ curves of *i*-AlCuFe quasicrystals can be consistently described in terms of the two-Lorentzian spectral conductivity function^{30,31}

$$\sigma(E) = \frac{B}{\pi} \left[\frac{\gamma_1}{(E-\delta_1)^2 + \gamma_1^2} + \alpha \frac{\gamma_2}{(E-\delta_2)^2 + \gamma_2^2} \right]^{-1}, \quad (12)$$

where B is a scale factor expressed in $\Omega^{-1} \text{ cm}^{-1} \text{ eV}^{-1}$ units, and the Lorentzian peaks are characterized by their height $(\pi \gamma_i)^{-1}$ and their position δ_i with reference to the Fermi level. The relative importance of the narrow and broad features in the overall electronic structure is expressed through the weight factor α . In addition, the γ_i parameters can be related to the diffusivity of the corresponding states.^{30,56} The reduced kinetic coefficients J_n corresponding to the $\sigma(E)$ function given by Eq. (12) can be expressed as⁵⁵

$$\begin{pmatrix} J_0 \\ J_1 \\ J_2 \end{pmatrix} = 4\sigma_0 \begin{pmatrix} 1 & 0 & \xi_2 & 0 & \xi_4 & 0 & j_0 \\ 0 & 2\xi_1 & 0 & 2\xi_3 & 0 & 2j_1 & 0 \\ \frac{\pi^2}{3} & 0 & \frac{\pi^2}{3} & \frac{21}{5}\xi_2 & 0 & \frac{\pi^2}{3}j_2 & 0 & 0 \end{pmatrix} \times \begin{pmatrix} 1 \\ \frac{bT}{k_B} \\ bT^2 \\ \frac{b^2 T^3}{k_B} \\ b^2 T^4 \\ \frac{b^3 T^5}{k_B} \\ b^3 T^6 \end{pmatrix}, \quad (13)$$

where $\sigma_0 = \sigma(T \rightarrow 0)$ is the residual electrical conductivity, and $b \equiv e^2 \mathcal{L}_0$. The phenomenological coefficients ξ_i , as well as the parametric functions $j_i = j_i(\xi_3, \xi_4)$, can be expressed in terms of the electronic model parameters $\{B, \alpha, \gamma_k, \delta_k\}$

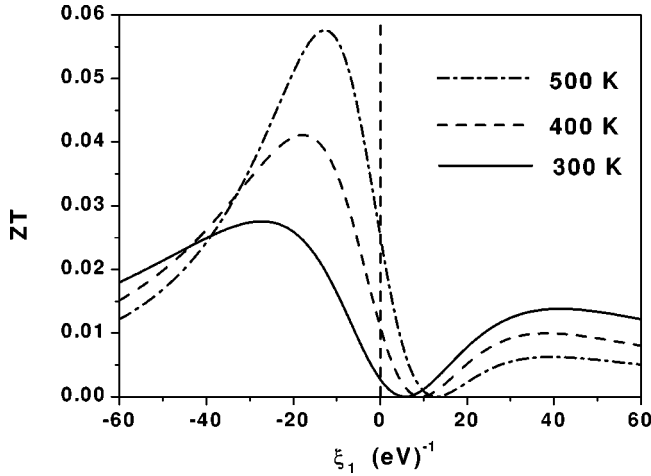


FIG. 5. Dependence of the thermoelectric figure of merit as a function of the phenomenological coefficient ξ_1 at $T=300$ K (solid line), $T=400$ K (dashed line), and $T=500$ K (dot-dashed line).

introduced in Eq. (12). The corresponding analytical expressions were fully derived in previous works.^{47,48,55} Making use of Eq. (13) in Eq. (11) we obtain

$$ZT = \frac{4bT^2P_1^2}{P_0(P_2 + \psi) - 4bT^2P_1^2}, \quad (14)$$

where $\psi(T) \equiv \varphi(T)/\sigma_0\mathcal{L}_0$, and we have introduced the polynomials

$$P_0(T) \equiv 1 + \xi_2 b T^2 + \xi_4 b^2 T^4 + j_0 b^3 T^6, \quad (15)$$

$$P_1(T) \equiv \xi_1 + \xi_3 b T^2 + j_1 b^2 T^4, \quad (16)$$

$$P_2(T) \equiv 1 + \frac{21}{5} \xi_2 b T^2 + j_2 b^2 T^4. \quad (17)$$

At a given temperature, Eq. (14) can be regarded as a parametric function of the different phenomenological coefficients, i.e., $ZT(\xi_i)$. Then, making use of the relationship $\xi_2 = 2\xi_1^2 + \Omega$, where

$$\Omega \equiv \frac{1}{2} \left(\frac{d^2 \ln \sigma(E)}{dE^2} \right)_{E=\mu}$$

measures the curvature of $\sigma(E)$ at the Fermi level,⁴⁷ we can express Eq. (14) in the form

$$ZT(\xi_1) = 4y \frac{(\xi_1 + F)^2}{K\xi_1^4 + G\xi_1^2 - 8yF\xi_1 + H}, \quad (18)$$

where $y \equiv bT^2$, $F \equiv \xi_3 y + j_1 y^2$, $K \equiv 84y^2/5$, $G \equiv 2y(21A/5 + C + \psi - 2)$, $A \equiv 1 + \Omega y + \xi_4 y^2 + j_0 y^3$, $C \equiv 1 + \frac{21}{5} \Omega y + j_2 y^2$, and $H \equiv A(C + \psi) - 4yF^2$.

In Fig. 5 we plot the ZT curve as a function of the ξ_1 value at different temperatures, as derived from Eq. (18), with $\kappa = 1.1 \text{ W m}^{-1} \text{ K}^{-1}$ (mean value of the values listed in Table II), $\sigma_0 = 30 (\Omega \text{ cm})^{-1}$ (mean value of the fitting analysis data reported in Ref. 57), $\Omega = 400 \text{ eV}^{-2}$ (cf. Ref. 47), $\xi_3 = -2910 \text{ eV}^{-3}$ (cf. Ref. 48), ξ_4

$= 17000 \text{ eV}^{-4}$ (cf. Ref. 48), $j_0 = 10^5 \text{ eV}^{-4}$, $j_1 = 130000 \text{ eV}^{-4}$, and $j_2 = -30000 \text{ eV}^{-4}$. In agreement with the empirical trends described in Sec. II, the $ZT(\xi_1)$ curve exhibits a deep minimum, where ZT almost vanishes, flanked by two maxima at about $\xi_1 \approx -25 \text{ eV}^{-1}$ and $\xi_1 \approx +40 \text{ eV}^{-1}$. Considering this curve by the light of Eq. (2), several conclusions can be drawn concerning the relationship between the ZT curves and the sample's electronic structure. First, when the Fermi level is located close to the pseudogap minimum, Eq. (2) yields very small ξ_1 values. In that case, Fig. 5 indicates that we will obtain small figures of ZT at room temperature, in agreement with the experimental results listed in Table III. Note, however, that the minimum of the $ZT(\xi_1)$ curve does not coincide with $\xi_1 = 0$, so that as the temperature is increased we obtain progressively larger values of ZT , in agreement with experimental findings as well. Second, as the Fermi level progressively shifts from the pseudogap's minimum, due to a systematic change in the sample stoichiometry, the ZT values progressively increase attaining well-defined maxima. Note that these maxima reach different peak values depending on the sign of ξ_1 . Accordingly, we conclude that best thermoelectric performances will be expected for those stoichiometries able to locate the Fermi level below the minimum of the pseudogap, and that the deeper the pseudogap, the larger the resulting FOM at a given temperature. Finally, we observe that as temperature increases, the $ZT(\xi_1)$ maximum below (above) the Fermi level progressively increases (decreases) and shifts towards (away from) the pseudogap's minimum located at $\xi_1 = 0$. This behavior indicates that the precise stoichiometry to get an optimal thermoelectric performance will depend, in general, on the working temperature for the considered sample.

IV. CONCLUSIONS

In this work we provide a theoretical analysis on the composition dependence of the FOM corresponding to i -AlPdRe samples at different working temperatures. To this end, we have considered a realistic model for the spectral conductivity which takes into account two main spectral features: a broad component (related to the Hume-Rothery mechanism) and a narrow component (related to sp - d hybridization mechanism and covalent bond formation). From our study we conclude that band-structure effects play a significant role in the thermoelectric performance of i -AlPdRe QC's (and likely in other quasicrystalline phases containing transition metals as well). In particular, we have shown the following.

(i) samples whose Fermi level is located at the pseudogap's minimum exhibit very small ZT values. This condition occurs for stoichiometries yielding $e/a \approx 1.74$. Thus, the most stable samples (e.g., $\text{Al}_{68.5}\text{Pd}_{22.9}\text{Re}_{8.6}$, $\text{Al}_{69.4}\text{Pd}_{21.2}\text{Re}_{9.4}$, $\text{Al}_{70}\text{Pd}_{20}\text{Re}_{10}$) are also the worse ones for thermoelectric applications. By inspecting Fig. 1 we realize that these samples are the only ones exhibiting negative Seebeck coefficient values at room temperature. This result suggests that good thermoelectric performance is associated with the nature of main charge carriers in QC's.

(ii) the absolute value of the phenomenological coefficient

ξ_1 , which measures the slope of the spectral conductivity function around the Fermi level, is directly correlated to the ZT value. Thus, large FOM values are expected for those samples exhibiting narrow features in the DOS close to the Fermi level, like i -Al_{70.5}Pd₂₁Re_{8.5}.^{26,27}

The high temperature dependence of the Seebeck coefficient of i -AlPdRe samples as a function of e/a was recently discussed by Kirihara and Kimura, concluding that the variation of the $S(e/a)$ curve arises from a combined effect involving a Fermi level shift and a deepening of the DOS pseudogap due to covalent bond formation.¹⁶ The results obtained in our work provide additional support to this view within the framework of a phenomenological approach. Consequently, it seems reasonable to expect that relatively high values of the FOM may be obtained by a judicious choice of

sample composition and working temperature. Our results favor high-temperature applications, in agreement with recent experimental studies, although the applicability of our rigid-band electronic structure model should be limited to temperatures below the Debye one.

ACKNOWLEDGMENTS

I warmly thank Professor K. Kimura, Professor R. Tamura, Professor T. M. Tritt, Dr. K. Kirihara, Dr. C. V. Landauro, and Dr. A. L. Pope for interesting comments and for sharing useful materials. I acknowledge M. V. Hernández for a critical reading of the manuscript. This work was supported by UCM through Project No. PR3/04-12450.

*Electronic address: emaciaba@fis.ucm.es

¹See, for example, T.M. Tritt, *Science* **283**, 804 (1999); **272**, 1276 (1996); F.J. DiSalvo, *ibid.* **285**, 703 (1999); G.D. Mahan and L.M. Woods, *Phys. Rev. Lett.* **80**, 4016 (1998); G. Mahan, B.C. Sales, and J. Sharp, *Phys. Today* **50**(1), 42 (1997), and references therein.

²G.A. Slack, *CRC Handbook of Thermoelectrics*, edited by D.M. Rowe (CRC Press, Boca Raton, FL, 1995).

³T.M. Tritt, A.L. Pope, M. Chernikov, M. Feuerbacher, S. Legault, R. Cagnon, and J. Strom-Olsen, in *Quasicrystals*, edited by J.M. Dubois, P. A. Thiel, A-P. Tsai, and K. Urban, MRS Symposia Proceedings No. 553 (Materials Research Society, Pittsburgh, 1999), p. 489; A.L. Pope, T.M. Tritt, M. Chernikov, M. Feuerbacher, S. Legault, R. Cagnon, and J. Strom-Olsen, in *Thermoelectric Materials 1998—The Next Generation Materials For Small-Scale Refrigeration and Power Generation Applications*, edited by T.M. Tritt, H.B. Lyon, Jr., G. Mahan, and M.G. Kanatzidis, MRS Symposia Proceedings No. 545 (Materials Research Society, Pittsburgh, 1999), p. 413.

⁴R. Tamura, A. Waseda, K. Kimura, and H. Ino, *Phys. Rev. B* **50**, 9640 (1994); T. Klein, C. Berger, D. Mayou, and F. Cyrot-Lackmann, *Phys. Rev. Lett.* **66**, 2907 (1991); A. Carlsson, *Nature* (London) **353**, 353 (1991).

⁵D. Mayou, C. Berger, F. Cyrot-Lackmann, T. Klein, and P. Lanco, *Phys. Rev. Lett.* **70**, 3915 (1993).

⁶A. Perrot and J.M. Dubois, *Ann. Chim. (Paris)* **18**, 501 (1993).

⁷B.D. Biggs, S.J. Poon, and N.R. Munirathnam, *Phys. Rev. Lett.* **65**, 2700 (1990); F.S. Pierce, S.J. Poon, and B.D. Biggs, *ibid.* **70**, 3919 (1993); B.D. Biggs, Y. Li, and S.J. Poon, *Phys. Rev. B* **43**, 8747 (1991); F.S. Pierce, P.A. Bancel, B.D. Biggs, Q. Guo, and S.J. Poon, *ibid.* **47**, 5670 (1993).

⁸R. Haberkens, G. Fritsch, and M. Härting, *Appl. Phys. A: Solids Surf.* **57**, 431 (1993); R. Haberkens, K. Khedhri, C. Madel, and P. Häussler, *Mater. Sci. Eng., A* **294-296**, 475 (2000).

⁹A. Bilušić, D. Pavuna, and A. Smontara, *Vacuum* **61**, 345 (2001); A. Bilušić, A. Smontara, J.C. Lasjaunias, J. Ivkov, and Y. Calvayrac, *Mater. Sci. Eng., A* **294-296**, 711 (2000).

¹⁰A.L. Pope, T.M. Tritt, M.A. Chernikov, and M. Feuerbacher, *Appl. Phys. Lett.* **75**, 1854 (1999).

¹¹S. Legault, B. Ellman, J.O. Ström-Olsen, L. Taillefer, S. Kycia, T. Lograsso, and D. Delaney, in *New Horizons in Quasicrystals: Research and Applications*, edited by A.I. Goldman, D.J. Sorde-

let, P.A. Thiel, and J.M. Dubois (World Scientific, Singapore, 1997), p. 224.

¹²M.A. Chernikov, A. Bianchi, and H.R. Ott, *Phys. Rev. B* **51**, 153 (1995); P.A. Kalugin, M.A. Chernikov, A. Bianchi, and H.R. Ott, *ibid.* **53**, 14 145 (1996).

¹³J.M. Dubois, S.S. Kang, P. Archambault, and B. Colletet, *J. Mater. Res.* **8**, 38 (1993); P. Archambault and C. Janot, *MRS Bull.* **22**, 48 (1997).

¹⁴K. Kirihara, T. Nakata, M. Takata, Y. Kubota, E. Nishibori, K. Kimura, and M. Sakata, *Phys. Rev. Lett.* **85**, 3468 (2000); K. Kirihara and K. Kimura, *Phys. Rev. B* **64**, 212201 (2001); K. Kirihara, T. Nagata, K. Kimura, K. Kato, M. Takata, E. Nishibori, and M. Sakata, *ibid.* **68**, 014205 (2003).

¹⁵A.L. Pope, B.M. Zawilski, R. Gagnon, T.M. Tritt, J. Ström-Olsen, R. Schneidmiller, and J.W. Kolis, in *Quasicrystals—Preparation, Properties and Applications*, edited by E. Belin-Ferré, P.A. Thiel, A-P. Tsai, and K. Urban, MRS Symposia Proceedings No. 643 (Materials Research Society, Pittsburgh, 2001), p. K14.4.1.

¹⁶K. Kirihara and K. Kimura, *J. Appl. Phys.* **92**, 979 (2002).

¹⁷T. Nagata, K. Kirihara, and K. Kimura, *J. Appl. Phys.* **94**, 6560 (2003).

¹⁸K. Kirihara, T. Nagata, and K. Kimura, *J. Alloys Compd.* **342**, 469 (2002).

¹⁹A.L. Pope, T.M. Tritt, R. Gagnon, and J. Strom-Olsen, *Appl. Phys. Lett.* **79**, 2345 (2001).

²⁰G.D. Mahan and J.O. Sofo, *Proc. Natl. Acad. Sci. U.S.A.* **93**, 7436 (1996).

²¹E. Maciá, *Appl. Phys. Lett.* **77**, 3045 (2000).

²²M.A. Chernikov, A. Bianchi, E. Felder, U. Gubler, and H.R. Ott, *Europhys. Lett.* **35**, 431 (1996).

²³M. Mori, S. Matsuo, T. Ishimasa, T. Matsuura, K. Kamiya, H. Inokuchi, and T. Matsukawa, *J. Phys.: Condens. Matter* **3**, 767 (1991).

²⁴E. Belin, Z. Dankhazi, A. Sadoc, Y. Calvayrac, T. Klein, and J.M. Dubois, *J. Phys.: Condens. Matter* **4**, 4459 (1992).

²⁵A. Shastri, F. Borsa, A.I. Goldman, J.E. Shield, and D.R. Torgeson, *J. Non-Cryst. Solids* **153&154**, 347 (1993); *Phys. Rev. B* **50**, 15 651 (1994).

²⁶R. Escudero, J.C. Lasjaunias, Y. Calvayrac, and M. Boudard, *J. Phys.: Condens. Matter* **11**, 383 (1999).

²⁷E. Maciá, *Phys. Rev. B* **69**, 132201 (2004).

- ²⁸F. Cyrot-Lackmann, in *Quasicrystals* (Ref. 3), p. 397; F. Cyrot-Lackmann, *Mater. Sci. Eng., A* **294-296**, 611 (2000).
- ²⁹E. Maciá, *Phys. Rev. B* **64**, 094206 (2001).
- ³⁰C.V. Landauro and H. Solbrig, *Mater. Sci. Eng., A* **294-296**, 600 (2000).
- ³¹H. Solbrig and C.V. Landauro, *Physica B* **292**, 47 (2000).
- ³²C.R. Lin, S.T. Lin, C.R. Wang, S.L. Chou, H.E. Horng, J.M. Cheng, Y.D. Yao, and S.C. Lai, *J. Phys.: Condens. Matter* **9**, 1509 (1997).
- ³³Y.K. Kuo, J.R. Lai, C.H. Huang, C.S. Lue, and S.T. Lin, *J. Phys.: Condens. Matter* **15**, 7555 (2003).
- ³⁴F.S. Pierce, Q. Guo, and S.J. Poon, *Phys. Rev. Lett.* **73**, 2220 (1994).
- ³⁵C. Gignoux, C. Berger, G. Fourcaudot, J.C. Grieco, and H. Rakoto, *Europhys. Lett.* **39**, 171 (1997).
- ³⁶J.J. Préjean, J.C. Lasjaunias, C. Berger, and A. Sulpice, *Phys. Rev. B* **61**, 9356 (2000).
- ³⁷A.D. Bianchi, F. Bommeli, M.A. Chernikov, U. Gubler, L. Degiorgi, and H.R. Ott, *Phys. Rev. B* **55**, 5730 (1997).
- ³⁸F.S. Pierce, S.J. Poon, and Q. Guo, *Science* **261**, 737 (1993).
- ³⁹Y. Honda, K. Edagawa, A. Yoshioka, T. Hashimoto, and S. Takeuchi, *Jpn. J. Appl. Phys.* **33**, 4929 (1994).
- ⁴⁰A.L. Pope, R. Schneidmiller, J.W. Kolis, T.M. Tritt, R. Gagnon, J. Strom-Olsen, and S. Legault, *Phys. Rev. B* **63**, 052202 (2001).
- ⁴¹F. Morales and R. Escudero, *Bull. Am. Phys. Soc.* **44**, 1 (1999).
- ⁴²K. Giannó, A.V. Sologubenko, L. Liechtenstein, M.A. Chernikov, and H.R. Ott, *Ferroelectrics* **250**, 249 (2001).
- ⁴³In general, the nominal composition would differ from the actual one, estimated from accurate techniques such as inductive-coupled plasma analysis (cf. Ref. 16). Since these fine analyses have been performed in very few cases, we will consider the less accurate nominal composition in order to provide an homogeneous treatment for all the considered samples.
- ⁴⁴G. Trambly de Laissardière, D.N. Manh, L. Magaud, J.P. Julien, F. Cyrot-Lackmann, and D. Mayou, *Phys. Rev. B* **52**, 7920 (1995).
- ⁴⁵G.V. Raynor, *Prog. Met. Phys.* **1**, 1 (1949).
- ⁴⁶A.P. Tsai, in *Physical Properties of Quasicrystals*, edited by Z.M. Stadnik, Springer Series in Solid-State Physics Vol. 126 (Springer-Verlag, Berlin, 1999), p. 5.
- ⁴⁷E. Maciá, *Phys. Rev. B* **66**, 174203 (2002).
- ⁴⁸E. Maciá, *J. Appl. Phys.* **93**, 1014 (2003).
- ⁴⁹X. Wu, S.W. Kycia, C.G. Olson, P.J. Benning, A.I. Goldman, and D.W. Lynch, *Phys. Rev. Lett.* **75**, 4540 (1995).
- ⁵⁰S. Roche and D. Mayou, *Phys. Rev. Lett.* **79**, 2518 (1997); S. Roche and T. Fujiwara, *Phys. Rev. B* **58**, 11 338 (1998).
- ⁵¹G.V. Chester and A. Thellung, *Proc. Phys. Soc. London* **77**, 1005 (1961).
- ⁵²D.A. Greenwood, *Proc. Phys. Soc. London* **71**, 585 (1958).
- ⁵³R. Kubo, *J. Phys. Soc. Jpn.* **12**, 570 (1957); R. Kubo, M. Yokota, and S. Nakajima, *ibid.* **12**, 1203 (1957).
- ⁵⁴E. Maciá, *Appl. Phys. Lett.* **81**, 88 (2002).
- ⁵⁵C.V. Landauro, E. Maciá, and H. Solbrig, *Phys. Rev. B* **67**, 184206 (2003).
- ⁵⁶C.V. Landauro, Ph.D. thesis, Technische Universität Chemnitz, 2002.
- ⁵⁷J. Delahaye, C. Berger, and G. Fourcaudot, *J. Phys.: Condens. Matter* **15**, 8753 (2003).